Electrochemical Oxidation of Methanol on Pt Nanoparticles Dispersed on RuO_2

H. Mercedes Villullas,* Flora I. Mattos-Costa, and Luis O. S. Bulhões

Departamento de Química, Universidade Federal de São Carlos, CMDMC - LIEC, C.P. 676, CEP: 13565-905, São Carlos - SP, Brazil

Received: January 23, 2004; In Final Form: June 20, 2004

Pt-modified RuO_2 was prepared by a sol−gel procedure on titanium substrates in the form of thin films of ~2-μm thickness. X-ray diffraction (XRD) and X-ray photoelectron spectroscopy (XPS) analyses showed that these films actually consist of Pt nanoparticles dispersed in RuO_2 and that neither metallic Ru nor Pt−Ru alloy are present on the surface. Electrodes with different Pt:Ru nominal compositions were prepared and their electrocatalytic activity for the oxidation of methanol was investigated by potential sweeps and chronoamperometry. The results obtained show an enhancement effect for methanol oxidation that can be interpreted as associated to the formation of hydrous oxides on the RuO_2 surface.

Introduction

Power generation using fuel cells has attracted so much attention because fuel cell systems are clean and silent, have high energy conversion efficiency, and can be used for stationary energy generation as well as for vehicles and portable devices.[1] Today, only hydrogen−oxygen fuel cells are capable of providing power densities for most practical applications. However, the use of hydrogen as fuel still involves production, storage, and distribution problems. Liquid fuels, such as methanol, are an attractive alternative because they can be stored and distributed more easily.

The oxidation of methanol has been investigated since the 1960s and continues to be one of the most studied reactions. Several reviews on methanol oxidation were published.[2−4] Pt is the most active electrocatalyst for the oxidation of small organic molecules such as methanol, but intermediate species such as CO remain adsorbed on the surface and inhibit the oxidation reaction. Significant efforts are being dedicated to the development of new electrocatalytic materials. Several different catalysts containing Pt with one or two other metals have been proposed for the oxidation of CO and organic compounds. Bimetallic systems such as Pt−Ru,[5−7] Pt−Sn,[7−9] Pt−W,[9,10] and Pt−Mo[10] have been studied. The oxidation of CO and methanol were studied on Pt−Ru catalysts prepared in various ways.[5−7,11−22] In all cases, an electrocatalytic effect associated with the presence of the Ru cocatalyst was observed. It is currently accepted that, to minimize the effect of the poisonous species, the cocatalyst must have a larger tendency to form oxides than Pt. Thus, the conversion of CO to CO_2 would be promoted by oxygenated species that form at lower potentials through the so-called bifunctional mechanism. Studies of the oxidation of CO on Pt and Pt−Ru alloys[23] have led to the conclusion that CO_2 formation occurs through a Langmuir−Hinshelwood mechanism. However, the nature and role of the superficial oxide species remain unclear. Some authors have suggested that the formation of ruthenium oxides may be the cause of the deactivation of Pt−Ru electrocatalysts,[19] while surface RuO_x species were observed on Pt−Ru/C anode catalysts by XPS analysis.[24] In addition, thermogravimetric analysis and XPS of some commercial Pt−Ru electrocatalysts has indicated substantial amounts of hydrous ruthenium oxide (RuO_xH_y).[25] It has been suggested that mixed-phase electrocatalyst containing Pt metal and hydrous ruthenium oxides (RuO_xH_y) would have better electrocatalytic activity and that bulk quantities of electron−proton conducting RuO_xH_y are required to achieve high activity for methanol oxidation.[25,26] A recent XANES study of as-prepared Pt−Ru materials showed that Pt and Ru were predominately in the form of oxides.[27] Additionally, in a recent study of Pt−Ru catalysts prepared at different temperatures by a modified Adams method it was concluded that the alloyed metallic Pt−Ru phase, as well as amorphous hydrated Ru oxides, favor the electrooxidation of methanol.[28] Improvement of the catalytic activity of Pt−Ru electrodes towards methanol electrooxidation has been reported for the introduction of transition metal oxides as cocatalysts.[29,30] In contrast, in a study carried out on Pt and Pt−Ru particles supported on RuO_2, no evidence of an enhancement effect was found[31] and it was concluded that RuO_2 does not meet the requirements to be an active support.

In this work, Pt-RuO_2/Ti electrodes were prepared by a sol−gel method and characterized by XRD and XPS as consisting of Pt nanoparticles and RuO_2. The electrocatalytic activity toward the oxidation of methanol was studied by potential sweeps and chronoamperometry for Pt−RuO_2/Ti electrodes of three different Pt:Ru nominal compositions.

Experimental Section

Pt−RuO_2 was prepared by a sol−gel process[32] in the form of thin films supported on titanium substrates, following a procedure similar to that described elsewhere.[33] Briefly, the sols were prepared by dissolving the precursors, chloroplatinic acid and ruthenium acetylacetonate (Aldrich), in alcohol followed by adding acetic acid and conducting an ultrasonic treatment. Sols containing different amounts of the precursors were prepared to obtain films with nominal Pt:Ru compositions (in atoms) of 20:80, 40:60, and 60:40. Aged sols were used to avoid high electrocatalytic activity toward oxygen evolution, as reported elsewhere.[33] The sols were brushed onto the Ti sheets (1 cm^2 of geometric area, previously sand blasted and cleaned

* Corresponding author. Present address: Instituto de Química, UNESP, 14800-900, Araraquara, SP, Brazil. E-mail: mercedes@iq.unesp.br.

10.1021/jp049662r CCC: $27.50
Published on Web 07/30/2004

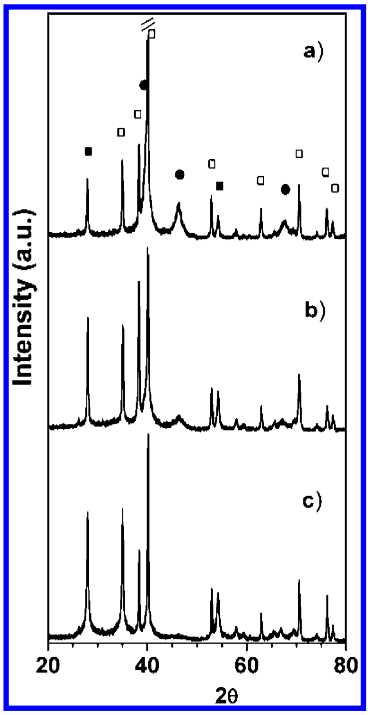

Figure 1. X-ray diffraction patterns for Pt−RuO_2/Ti electrodes of different nominal Pt:Ru composition. (a) 60:40, (b) 40:60, and (c) 20:80. Symbols: (●) metallic Pt, (■) RuO_2, and (□) Ti.

with hot oxalic acid solution) under a flux of hot air to promote the formation of the xerogel film. This film was then heated in a preheated furnace for 5 min. This procedure was repeated several times until a nominal thickness of about 2 μm was reached. A final heat treatment at 400 °C in air was done to promote densification and elimination of any unreacted residues. For comparison purposes, in some cases the xerogel film was submitted to the final densification heat treatment in a H_2 atmosphere. Thus, during the densification step the xerogel was also reduced to make an "all metallic" Pt−Ru layer.

X-ray diffraction measurements were done with a Rigaku D Max 2500 PC X-ray diffractometer using a wavelength of 1.5406 Å (KαCu) and using a fixed angle of incidence of 2°. The X-ray photoelectron spectroscopy (XPS) analysis was performed using a Kratos Analytical XSAM HS spectrometer, with an Al Kα ($h\nu$ = 1486.6 eV) X-ray source. The binding energies were referred to the adventitious hydrocarbon C 1s line set at 284.8 eV. Gaussian line shapes were used to fit the curves for C 1s and O 1s, and a mixed Gaussian/Lorentzian function was employed for Pt 4f and Ru 3d. The Shirley background and a least-squares routine were used for fitting of the peaks. The sensitivity factors for quantitative analysis were referenced to SF1s = 1.0.

All the electrochemical measurements were carried out in a conventional electrochemical cell, with a Pt foil counterelectrode placed in a separate compartment and a reversible hydrogen reference electrode. Solutions were prepared from analytical grade reagents (Merck) and ultrapure water. All experiments were done at room temperature in nitrogen saturated solutions.

Results and Discussion

Composition of the Sol−Gel Layers. The bulk constituents of the sol−gel prepared Pt-modified RuO_2 layers were determined by X-ray diffraction. Even though a small angle technique was employed, all the diffraction spectra showed diffraction signals produced by the Ti substrate. Figure 1 shows the

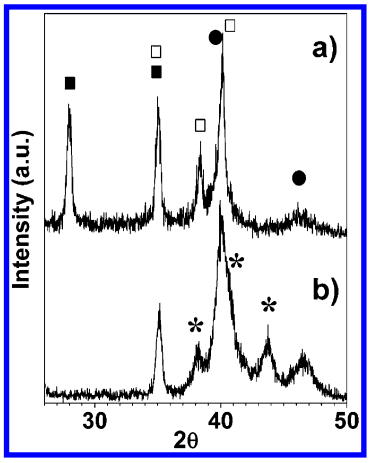

Figure 2. X-ray diffraction patterns: (a) Pt−RuO_2/Ti electrode (Pt:Ru 40:60), (b) hydrogen-reduced electrode with the same nominal composition. Symbols: (●) metallic Pt, (■) RuO_2, (□) Ti, and (*) metallic Ru.

diffraction patterns obtained for Pt-modified RuO_2 electrodes of nominal Pt:Ru compositions of 60:40, 40:60, and 20:80. As can be seen, variation of the nominal composition of electrodes did not produce significant changes in the XRD patterns, other than the expected variations of relative intensities of the peaks. The diffraction peak at $2\theta = 28°$ corresponds to the most intense diffraction peak of RuO_2 (JCPDS 43-1027 and 40-1290).

Even though the main diffraction peak of Pt (2θ = 39.8°, JCPDS 04-802) overlaps with the main diffraction peak of the Ti substrate (2θ = 40.1°, JCPDS 44-1294), the presence of metallic platinum is clearly revealed by the characteristic diffraction peaks of the Pt [200] and [220] planes at 2θ values of 46.2 and 67.4°, respectively. The peak at $2\theta = 46.2°$ was used to calculate the mean size of the Pt nanoparticles using Scherrer's equation, assuming that the particles are spherical.[34] The average size of the Pt nanoparticles was found to be 5.5 and 4.2 nm for the Pt:Ru 60:40 and 40:60 electrodes, respectively. These particle size values are in good agreement with those reported for nanoparticulated Pt obtained by a sol−gel derived process and heat treated at 400 °C.[35] For the Pt:Ru 20:80 electrode the average size of the Pt nanoparticles cannot be accurately calculated. The average sizes of RuO_2 nanoparticles were found to be 24, 38.6, and 34 nm for the 20:80, 40:60, and 60:40 electrodes, respectively, in good agreement with recently reported values for RuO_2 prepared under similar conditions.[36]

In summary, it can be said that according to XRD analysis these materials actually consist of Pt nanoparticles and RuO_2. Further evidence is obtained by comparing the XRD pattern of a Pt−RuO_2/Ti electrode and that of a sample of identical nominal composition reduced in H_2, as shown in Figure 2. As can be seen, the main diffraction peak of RuO_2 observed at $2\theta = 28°$ in the pattern of the Pt-RuO_2/Ti electrode (Figure 2a) is completely absent in the pattern of the H_2-treated sample (Figure 2b). In addition, the Pt characteristic peak of the [200] is observed at a 2θ value that coincides with the tabulated value of 46.2° in the pattern of the Pt−RuO_2/Ti sample while in that of the hydrogen reduced layer the diffraction peak of the Pt [200] planes is shifted to $2\theta = 46.5°$. Diffraction patterns for PtRu catalysts reported in the literature usually exhibit Pt diffraction peaks at 2θ values greater than those of pure Pt. Since, according to Vegard's law the crystal lattice contracts if the material forms a solid solution with atoms of smaller radii, this shift is interpreted as caused by the incorporation of Ru in the Pt fcc structure and taken as evidence of the formation of a PtRu alloy.[24] Two additional signals are apparent in the

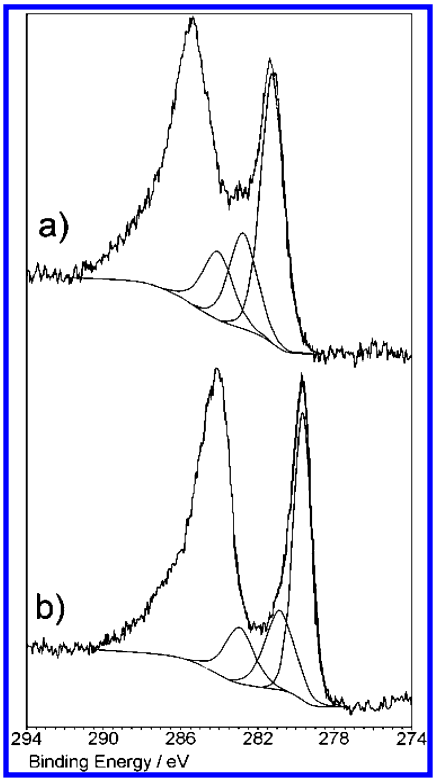

Figure 3. Ru 3d + C 1s high-resolution XP spectra. (a) Pt−RuO_2/Ti electrode (Pt:Ru 40:60), (b) hydrogen-reduced electrode with the same nominal composition. (For clarity, only the fits for Ru $3d_{5/2}$ lines are shown).

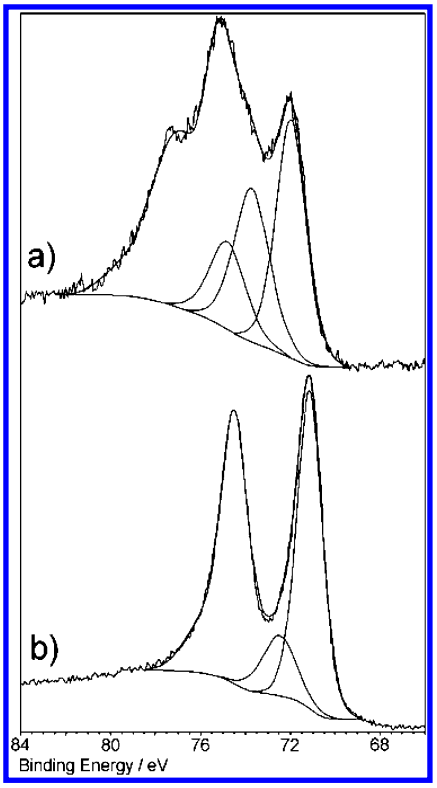

Figure 4. Pt 4f high-resolution XP spectra. (a) Pt−RuO_2/Ti electrode (Pt:Ru 40:60), (b) hydrogen-reduced electrode with the same nominal composition. (Only fits for Pt $4f_{7/2}$ lines are shown, for clarity).

diffractogram of the H_2 reduced layer, one at a 2θ of about 41° that is not well defined because of the partial overlap with Ti and Pt signals, and another at $2\theta = 43.7°$ that can be attributed to metallic Ru (JCPDS 06-0663). The latter signal can be assigned to the 100% intensity diffraction peak of Ru, shifted toward a smaller 2θ value in relation to the tabulated 44.01° for the [101] planes of pure Ru. Altogether, the XRD data show that neither metallic Ru nor Pt−Ru alloy are present in the Pt−RuO_2/Ti electrode.

XPS analyses were performed on as-prepared samples. Wide-range XP spectra indicated that the surfaces were free from contamination with Ti or chloride. Detailed scans were recorded for the Pt 4f, Ru 3d, O 1s, and C 1s regions. Figure 3a shows the Ru 3d + C 1s spectra for a Pt−RuO_2/Ti electrode. The spectrum was deconvoluted into three components with binding energies of 281.1, 282.7, and 284 eV. To facilitate the assignment of the near-surface Ru species of the Pt−RuO_2/Ti sample, Figure 3b shows the Ru 3d + C 1s spectra obtained for the H_2 reduced sample. The line that has its major intensity centered at 279.8 eV can be assigned to Ru metal.[37] The component with a binding energy of 281 eV can be attributed to RuO_2 and the photoelectron intensity above 282 eV would correspond to Ru−O speciation.[37] By comparing the photoelectron spectra of Figure 3a and Figure 3b, it becomes quite clear that the components of the XP spectrum of the Pt−RuO_2/Ti sample (Figure 3a) can be assigned to ruthenium oxides *but not to Ru metal*. In fact, this should not be surprising since published results for RuO_2[36] and RuO_2-containing mixtures[38] prepared by similar methods showed no photoelectron intensity corresponding to zero-valence Ru and binding energies of 281 eV ($3d_{5/2}$) and 285 eV ($3d_{3/2}$) that were attributed to RuO_2. The signal of the Ru 3d XP-spectrum of the Pt−RuO_2/Ti sample (Figure 3a) at 281 eV can be assigned to RuO_2 and the two others (282.7 and 284 eV) can be assigned to either RuO_3 and RuO_4[39] or to hydrous speciation RuO_xH_y.[25]

To give a definite interpretation of these peak components is beyond the scope of this work. What really matters to this work is that the Ru 3d spectra obtained for the Pt−RuO_2/Ti electrode (Figure 3a) proves the absence in the near-surface of ruthenium in the zero-valence state and, therefore, indicates that no Pt−Ru alloy is present in the Pt−RuO_2/Ti electrode, in agreement with the XRD data.

The Pt 4f XP spectrum for the Pt−RuO_2/Ti electrode is presented in Figure 4a, and that of the H_2-reduced sample is shown in Figure 4b, for comparison. The sole shape of the spectrum in the Pt 4f region for the Pt−RuO_2/Ti electrode already suggests a significant amount of metal oxide species. This spectrum was deconvoluted into three doublets with binding energies of 71.8, 73.6, and 74.7 eV. The line with major intensity centered at 71.8 eV can be assigned to Pt in the zero-valence metallic state, shifted toward higher values with respect to the 71.2 eV from literature.[37] In fact, peak shifts toward higher values of binding energies for the Pt $4f_{7/2}$ in relation to pure Pt have been reported for carbon-supported[40] and zeolite-supported Pt,[41] and they have been interpreted as caused by Pt-support interactions. Similarly, the observed shift toward higher binding energies could be interpreted in terms of interactions of Pt with the ruthenium oxide matrix in which the Pt nanoparticles are dispersed. The peak components at 73.6 and 74.7 eV can be assigned to Pt^{2+} and Pt^{4+} species.[37] The O 1s photoelectron spectrum for the Pt−RuO_2/Ti sample (not shown) was composed of species with binding energies that can be attributed to oxide oxygen (530.1 eV, typical value of transition metal oxides), to hydroxides (531.6 eV), and to hydration or adsorbed water (532.9 eV).[38] Regarding the Pt/Ru ratio, a Pt surface enrichment (∼10−15% higher than the nominal composition) was observed.

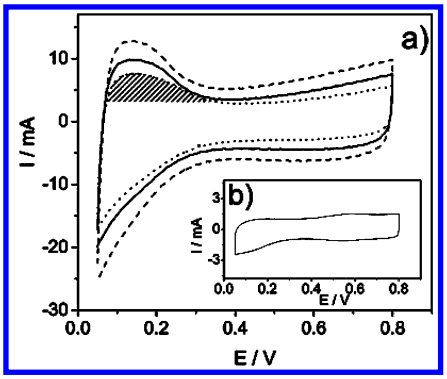

Figure 5. (a) Voltammetric curves taken at 50 mV s^{-1} between 0.05 and 0.8 V for Pt−RuO_2/Ti electrodes of different compositions. Pt percentage: (−−−) 20, (—) 40, and (···) 60. Electrolyte: 1 mol L^{-1} $HClO_4$. The shaded area represents the charge attributed to hydrogen desorption. (b) Voltammetric curve of a RuO_2/Ti electrode (preparation procedure as for the Pt−RuO_2/Ti electrodes). All experimental conditions as in part a.

Cyclic Voltammetry of Pt−RuO_2/Ti Electrodes. The voltammetric curves obtained for the as-prepared Pt−RuO_2/Ti electrodes of three different nominal compositions in 1 mol L^{-1} $HClO_4$ acid solution at 50 mV s^{-1} in the potential range of 0.05−0.8 V are shown in Figure 5a. The total charges involved in the voltammetric curves depend on the electrode composition and decrease as the content of Pt increases. In a general manner, these curves are very similar to those of Pt catalysts supported on carbon[21] or oxides, such as SnO_2[42] and IrO_2,[43] in the same potential window.

Even though crystalline anhydrous RuO_2 is rapidly and reversibly oxidized and reduced by electrochemical protonation[44]

$$RuO_2 + \delta H^+ + \delta e^- \leftrightarrow RuO_{2-\delta}(OH)_\delta,\ 0 \le \delta \le 2 \quad (1)$$

with the Ru in a valence state $Ru^{2+}(OH)_2$ at about 0 V (vs SHE), increasing to $Ru^{4+}O_2$ at about 1.4 V, it is well-known that the cyclic voltammetry of RuO_2 shows currents nearly independent of potential, with little evidence of the redox transitions Ru^{2+}/Ru^{3+} and Ru^{3+}/Ru^{4+}, as shown in Figure 5b. This implies that a pseudocapacitance is, in principle, the only expected contribution of RuO_2 in practically the whole potential window of Figure 5a (0.05−0.8V).

The anodic charge of the curves of Figure 5a was integrated up to ∼0.35 V, after accounting for the double-layer contribution as indicated by the shaded area in the figure. In situ X-ray diffraction[45] and XPS[46,47] experiments have demonstrated that RuO_2 is not electrochemically reduced to metallic ruthenium, even under hydrogen evolution conditions. Since hydrogen is not adsorbed onto ruthenium oxide,[48] these charges can be taken as due to the desorption of the hydrogen adsorbed on the Pt nanoparticles, and they lead to ratios of the active/geometric Pt area of 71, 95, and 106 for the 60:40; 40:60, and 20:80 Pt−RuO_2/Ti electrodes, respectively.

Electrocatalysis of Methanol Oxidation. Cyclic voltammograms for methanol oxidation on the Pt−RuO_2/Ti electrodes were obtained in the potential range between 0.05 and 0.9 V in solutions containing 0.5 mol L^{-1} methanol in 1 mol L^{-1} $HClO_4$ acid. Some curves obtained at sweep rates of 10 mV s^{-1} are shown in Figure 6. As can be seen in Figure 6a, during the positive-going scan the current increases rapidly until a current peak is seen. After reversing the potential, a reactivation is observed on all three electrodes. For all of the electrodes, the

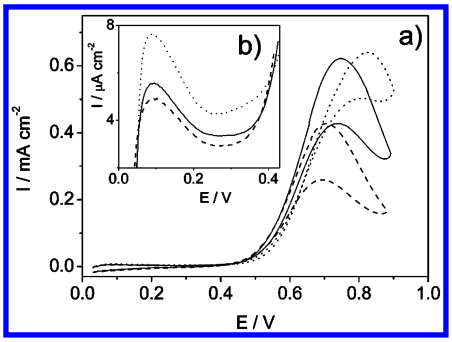

Figure 6. (a) Voltammetric curves taken at 10 mV s^{-1} between 0.05 and 0.9 V for Pt−RuO_2/Ti electrodes of different compositions. Pt percentage: (−−−) 20, (—) 40, and (···) 60. Electrolyte: methanol 0.5 mol L^{-1} in 1 mol L^{-1} $HClO_4$. (b) Initial parts of the curves of Figure 6a.

current peak observed during the negative-going potential scan is slightly shifted toward more negative potential in relation to the peak of the positive-going sweep. Even though the general features of the voltammetric curves are somewhat similar, it is evident that the electrode composition has a significant influence on the behavior toward methanol oxidation. The rise in current is initially faster for the 20:80 Pt−RuO_2/Ti electrode, which exhibits the highest currents at potentials below ca. 0.6 V. Peak potentials are strongly dependent on the electrode composition and shift to more positive potentials as the Pt content increases. It must also be mentioned that intense bubble formation occurred in the course of these experiments. In a general manner, the voltammetric curves shown in Figure 6a look like those published for Pt−Ru alloys.[49] The onset potential of the reaction is ∼0.3 V (Figure 6b). This potential value is close to those reported in the literature for methanol oxidation on Pt−Ru alloys.

The electrochemical behavior of RuO_2 and RuO_2-based materials has been thoroughly studied because they are attractive candidates for a variety of technological applications.[44,50] Some important fundamental properties of RuO_2 electrodes, such as the mechanism of electrical conduction, the hydration of the oxide layer, and the oxide layer's ability to exchange protons with the solution are fairly well understood.[44,50] Reaction 1 and its rate were experimentally determined by tritium exchange experiments by G. Lodi et al. in 1978.[51] The hydrogenated oxide $RuO_{2-\delta}(OH)_\delta$ (also written in the literature as RuO_xH_y or $RuO_2.xH_2O$) is a mixed electron/proton conductor, is able to dissociate water, and has surface Ru-OH bonds.

As mentioned in the Introduction section, Rolison and co-workers[25,26] have suggested that bulk quantities of electron−proton conducting RuO_xH_y would be necessary to achieve high activity for methanol oxidation. Hydrogenated ruthenium oxide species $RuO_{2-\delta}(OH)_\delta$ would be expected to form on the RuO_2 component of the Pt−RuO_2/Ti electrode surface and hence the enhancement effects observed could be interpreted as proposed by Rolison and co-workers,[25,26] that is, in terms of $RuO_{2-\delta}(OH)_\delta$ species that would be able to facilitate the conversion of CO to CO_2. In that context, the differences in the performance of electrodes with different compositions could be interpreted in terms of a balance between the amount of Pt sites where dehydrogenation and oxidation of methanol takes place, that is, the sites where the dissociative chemisorption of methanol occurs, and the amount of $RuO_{2-\delta}(OH)_\delta$ available for the CO to CO_2 conversion.

Chronoamperometric curves obtained at 0.5 V for Pt−RuO_2/Ti electrodes of different compositions are shown in Figure 7. First, a potential step from the open circuit potential (∼0.03 V)

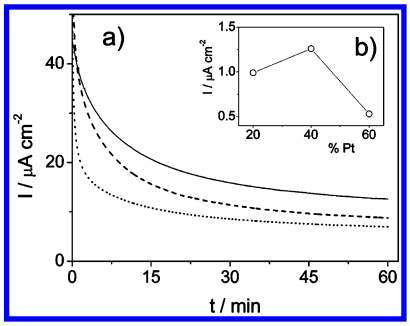

Figure 7. (a) Current density−time curves at 0.5 V for Pt−RuO_2/Ti electrodes of different compositions. Pt percentage: (−−−) 20, (−) 40, and (···) 60. Electrolyte: methanol 0.5 mol L^{-1} in 1 mol L^{-1} $HClO_4$. (b) Current density after 50 min polarization at 0.5 V against Pt percentage.

to 0.1 V was applied immediately after introducing the electrode in the solution. After waiting 30 s at 0.1 V, the potential was then stepped to 0.5 V and the current−time curve was recorded. For all the Pt−RuO_2/Ti electrodes, a pronounced decay of the current density is observed at the beginning of the curves. During the first 10 min of the measurement, the current decreases by a factor of c.a. 4−5. This decrease is more pronounced for the electrode with the highest Pt content. During the following 50 min of the experiment, the current decay is slower and the current density seems to evolve toward a steady-state value. The values of current density measured on the Pt−RuO_2/Ti electrodes depend on the composition, as shown in Figure 7b where the current density measured after 50 min of polarization at 0.5 V is plotted against platinum percentage. Similar current decays during potentiostatic measurements have been reported for smooth Pt−Ru catalysts[19,52,53] and for porous electrodes.[22] Even though some authors have postulated the formation of RuO_2 among the possible causes for the deactivation of alloys and other Pt−Ru catalysts,[19] the reasons for this type of deactivation are still unknown.

In principle, the essence of the bifunctional mechanism does not change by substituting Ru for a hydrous ruthenium oxide component, as already pointed out by Rolison et al.,[25] but whether the $RuO_{2-\delta}(OH)_\delta$ species are promoting the conversion of CO to CO_2 through a bifunctional mechanism remains, at this point, unclear. What seems clear, though, is that the mechanistic understanding of methanol oxidation and the nature and role of oxygenated species need to be readdressed.

Conclusions

It has been shown that Pt−RuO_2/Ti electrodes prepared by a sol−gel method and treated in air at 400 °C are actually formed by Pt nanoparticles and RuO_2. XPS analyses also show that neither metallic Ru nor Pt−Ru alloy are present on the surface. Pt−RuO_2/Ti electrodes exhibit an enhancement effect for the oxidation of methanol that can be interpreted as being associated with the presence of hydrous ruthenium oxide ($RuO_{2-\delta}(OH)_\delta$), which would play the role of donor of the oxygen-containing species that promote the CO to CO_2 oxidation.

Acknowledgment. The authors are indebted to Prof. P. A. P. Nascente (Departamento de Engenharia de Materiais, Universidade Federal de São Carlos) for the XPS analyses. Thanks are due to Fundação de Amparo à Pesquisa do Estado de São Paulo (FAPESP) and to Conselho Nacional de Desenvolvimento Científico e Tecnológico (CNPq) for financial support. H.M.V. and F.I.M.C. thank CNPq for the research fellowships granted.

References and Notes

(1) Carrette, L.; Fiedrich, K. A.; Stimming, U. *Fuel Cells* **2001**, *1*, 5−39.
(2) Iwasita, T. In *Advances in Electrochemical Science and Engineering*; Gerischer H.; Tobias, C., Eds.; Verlag Chemie, 1990; Vol. 1, pp. 127−170.
(3) Hamnett, A. In *Interfacial Electrochemistry. Theory, Experimental and Applications*; Wieckowski, A., Ed.; Marcel Dekker: New York, 1999, Chapter 47.
(4) Iwasita, T. *Electrochim. Acta* **2002**, *47*, 3663−3664.
(5) Gasteiger, H. A.; Markovic, N.; Ross, P. N.; Cairns, E. J. *J. Phys. Chem.* **1993**, *97*, 12020−12029.
(6) Krausa, M.; Vielstich, W. *J. Electroanal. Chem.* **1994**, *379*, 307−314.
(7) Arico, A. S.; Poltarzewski, Z.; Kim, H.; Morana, A.; Giordano, N.; Antonucci, V. *J. Power Sources* **1995**, *55*, 159−166.
(8) Wang, K.; Gasteiger, H. A.; Markovic, N.; Ross, P. N. *Electrochim. Acta* **1996**, *41*, 2587−2593.
(9) Gotz, M.; Wendt, H. *Electrochim. Acta* **1998**, *43*, 3637−3644.
(10) Oliveira-Neto, A.; Perez, J.; Napporn, W. T.; Ticianelli, E. A.; Gonzalez, E. R. *J. Brazil. Chem. Soc.* **2000**, *11*, 39−43.
(11) Gasteiger, H. A.; Markovic, N.; Ross, P. N.; Cairns, E. J. *J. Electrochem. Soc.* **1994**, *141*, 1795−1803.
(12) Markovic, N.; Gasteiger, H. A.; Ross, P. N.; Jiang, X. D.; Villegas, L.; Weaver, M. J. *Electrochim. Acta* **1995**, *40*, 91−95.
(13) Watanabe, M.; Uchida, M.; Motoo, S. *J. Electroanal. Chem.* **1987**, *229*, 395−406.
(14) Chrzanowski, W.; Wieckowski, A. *Langmuir* **1998**, *14*, 1967−1970.
(15) Chrzanowski, W.; Kim, H.; Wieckowski, A. *Catal. Lett.* **1998**, *50*, 69−75.
(16) Kabbabi, A.; Faure, R.; Durand, R.; Beden, B.; Hahn, F.; Leger, J. M.; Lamy, C. *J. Electroanal. Chem.* **1998**, *444*, 41−53.
(17) Kelley, S. C.; Deluga, G. A.; Smyrl, W. H. *Electrochem. Solid-State Lett.* **2000**, *3*, 407−409.
(18) Iwasita, T.; Hoster, H.; John-Anacker, A.; Lin, W. F.; Vielstich, W. *Langmuir* **2000**, *16*, 522−529.
(19) Hoster, H.; Iwasita, T.; Baumgartner, H.; Vielstich, W. *Phys. Chem. Chem. Phys.* **2001**, *3*, 337−346.
(20) Kardash, D.; Korzeniewski, C.; Markovic, N. *J. Electroanal. Chem.* **2001**, *500*, 518−523.
(21) Lizcano-Valbuena, W. H.; Paganin, V. A.; Gonzalez, E. R. *Electrochim. Acta* **2002**, *47*, 3715−3722.
(22) Bonnemann, H.; Brinkmann, R.; Britz, P.; Endruschat, U.; Mortel, R.; Paulus, U. A.; Feldmeyer, G. J.; Schmidt, T. J.; Gasteiger, H. A.; Behm, R. J. *J. New Mater. Electrochem. Systems* **2000**, *3*, 199−206.
(23) Gasteiger, H. A.; Markovic, N.; Ross, P. N.; Cairns, E. J. *J. Phys. Chem.* **1994**, *98*, 617−625.
(24) Arico, A. S.; Creti, P.; Kim, H.; Mantegna, R.; Giordano, N.; Antonucci, V. *J. Electrochem. Soc.* **1996**, *143*, 3950−3959.
(25) Rolison, D. R.; Hagans, P. L.; Swider, K. E.; Long, J. W. *Langmuir* **1999**, *15*, 774−779.
(26) Long, J. W.; Stroud, R. M.; Swider-Lyons, K. E.; Rolison, D. R. *J. Phys. Chem. B* **2000**, *104*, 9772−9776.
(27) O'Grady, W. E.; Hagans, P. L.; Pandya, K. I.; Maricle, D. L. *Langmuir* **2001**, *17*, 3047−3050.
(28) Lasch, K.; Jorissen, L.; Friedrich, K. A.; Garche, J. *J. Solid State Electrochem.* **2003**, *7*, 619−625.
(29) Lasch, K.; Jorissen, L.; Garche, J. *J. Power Sources* **1999**, *84*, 225−230.
(30) Jusys, Z.; Schmidt, T. J.; Dubau, L.; Lasch, K.; Jorissen, L.; Garche, J.; Behm, R. J. *J. Power Sources* **2002**, *105*, 297−304.
(31) Lasch, K.; Hayn, G.; Jörissen, L.; Garche J.; Besenhardt, O. *J. Power Sources* **2002**, *105*, 305−310.
(32) Brinker, C. J.; Scherer G. W. *Sol gel science. The physics and chemistry of sol gel processing*; Academic Press: San Diego, 1990.
(33) Villullas, H. M.; Mattos Costa, F. I.; Bulhões, L. O. S. *J. Electroanal. Chem.* **2003**, *545*, 89−97.
(34) West, A. R. *Solid State Chemistry and Its Applications*; Wiley: Chichester, 1984.
(35) Andreas, H. A.; Birss, V. I. *J. Electrochem. Soc.* **2002**, *149*, A1481−A1488.
(36) Armelao, L.; Barreca, D.; Moraru, B. *J. Non-Cryst. Solids* **2003**, *316*, 364−371.
(37) Moulder, J. F.; Stikle, W. F.; Sobol, P. E.; Bomben, K. D. *Handbook of X-ray Photoelectron Spectroscopy*; Perkin-Elmer: 1992.
(38) Kodintsevt, I. M.; Trasatti, S.; Rubelt, M.; Wieckowski, A.; Kaufher N. *Langmuir* **1992**, *8*, 283−290.
(39) Liu, R.; Iddir, H.; Fan, Q.; Hou, G.; Bo, A.; Ley, K. L.; Smotkin, E. S.; Sung, Y. E.; Kim, H.; Thomas, S.; Wieckowski, A. *J. Phys. Chem. B* **2000**, *104*, 3518−3531.
(40) Antolini, E.; Giorgi, L.; Cardellini, F.; Passalacqua, E. *J. Solid State Electrochem.* **2001**, *5*, 131−140.

(41) Vedrine, J. C.; Dufaux, M.; Naccache, C.; Imelik, B. *J. Chem. Soc., Faraday Trans*. **1978**, *74*, 440−449.

(42) Villullas, H. M.; Mattos-Costa, F. I.; Bulhões, L. O. S. *Electrochim. Acta* (in press).

(43) Mattos-Costa, F. I.; Villullas, H. M.; Bulhões, L. O. S. Unpublished results.

(44) Trasatti, S.; Lodi, G. In *Electrodes of Conductive Metallic Oxides − Part A*, Trasatti, S., Ed.; Elsevier: New York, 1980; pp 301−358.

(45) Chabanier, C.; Irissou, E.; Guay, D.; Pelletier, J. F.; Sutton, M.; Lurio, L. B. *Electrochem. Solid-State Lett.* **2002**, *5*, E40−E42.

(46) Blouin, M.; Guay, D. *J. Electrochem. Soc.* **1997**, *144*, 573−581.

(47) Rochefort, D.; Dabo, P.; Guay, D.; Sherwood, P. M. A. *Electrochim. Acta* **2003**, *48*, 4245−4252.

(48) Chu, Y. S.; Lister, T. E.; Cullen, W. G.; You, H.; Nagy, Z. *Phys. Rev. Letter* **2001**, *86*, 3364−3367.

(49) Tripkovic, A. V.; Popovic, K. D.; Grgur, B. N.; Blizanac, B.; Ross, P. N.; Markovic, N. M. *Electrochim. Acta* **2002**, *47*, 3707−3714.

(50) Trasatti, S. *Electrochim. Acta* **1991**, *36*, 225−241.

(51) Lodi G.; Zucchini, G.; De Battisti A.; Sivieri, E.; Trasatti, S. *Mater. Chem*. **1978**, *3*, 179−188.

(52) Waszczuk, P.; Solla-Gullón, J.; Kim, H.-S.; Tong, Y. Y.; Montiel, V.; Aldaz, A.; Wieckowski, A. *J. Catal*. **2001**, *203*, 1−6.

(53) Waszczuk, P.; Lu, G.-Q.; Wieckowski, A.; Lu, C. Rice, C.; Masel, R. I. *Electrochim. Acta* **2002**, *47*, 3637−3652.